Naval Research Laboratory
Washington, DC 20375-5320

NRL/MR/7631--19-9836

The Navy-Highly Integrated Thermosphere Ionosphere Demonstration System (Navy-HITIDES): Purpose, Design and Use

Fabrizio Sassi, Sarah E. McDonald, Christopher Metzler, Douglas Drob, Katherine Zawdie, John McCormack and Christoph R. Englert

Geospace Science & Technology Branch
Space Science Division

Jennifer Tate

Computational Physics, Inc.
Springfield, VA

April 10, 2019

REPORT DOCUMENTATION PAGE

Form Approved
OMB No. 0704-0188

1. REPORT DATE *(DD-MM-YYYY)*
10-04-2019

2. REPORT TYPE
Memorandum Report

3. DATES COVERED *(From - To)*
October 2014 - September 2018

4. TITLE AND SUBTITLE

The Navy-Highly Integrated Thermosphere Ionosphere Demonstration System (Navy-HITIDES): Purpose, Design and Use

5a. CONTRACT NUMBER

5b. GRANT NUMBER

5c. PROGRAM ELEMENT NUMBER

6. AUTHOR(S)

Fabrizio Sassi, Sarah E. McDonald, Jennifier Tate*, Christopher Metzler, Douglas Drob, Katherine Zawdie, John P. McCormack, and Christoph R. Englert

5d. PROJECT NUMBER

5e. TASK NUMBER

5f. WORK UNIT NUMBER

7. PERFORMING ORGANIZATION NAME(S) AND ADDRESS(ES)

Naval Research Laboratory
4555 Overlook Avenue, SW
Washington, DC 20375-5320

8. PERFORMING ORGANIZATION REPORT NUMBER

NRL/MR/7631--19-9836

9. SPONSORING / MONITORING AGENCY NAME(S) AND ADDRESS(ES)

Naval Research Laboratory
4555 Overlook Avenue, SW
Washington, DC 20375-5320

10. SPONSOR / MONITOR'S ACRONYM(S)

NRL

11. SPONSOR / MONITOR'S REPORT NUMBER(S)

12. DISTRIBUTION / AVAILABILITY STATEMENT

DISTRIBUTION STATEMENT A: Approved for public release; distribution is unlimited.

13. SUPPLEMENTARY NOTES

*Computational Physics, Inc., 8001 Braddock Road, Suite 210, Springfield, VA 22151-2110

14. ABSTRACT

This report describes the technical approach and implementation of atmosphere/ionosphere coupling in Navy-HITIDES. The document has a dual use: it is intended to be a general reference for users of Navy-HITIDES, while also providing documentation of the strategy used in order to achieve the final product.

15. SUBJECT TERMS

Thermosphere-ionosphere coupling
Whole atmosphere modeling

16. SECURITY CLASSIFICATION OF: a. REPORT	b. ABSTRACT	c. THIS PAGE	17. LIMITATION OF ABSTRACT	18. NUMBER OF PAGES	19a. NAME OF RESPONSIBLE PERSON
Unclassified Unlimited	Unclassified Unlimited	Unclassified Unlimited	Unclassified Unlimited	44	Fabrizio Sassi
					19b. TELEPHONE NUMBER *(include area code)* (202) 767-3827

Standard Form 298 (Rev. 8-98)
Prescribed by ANSI Std. Z39.18

This page intentionally left blank.

CONTENTS

This page intentionally left blank.

The Navy-Highly Integrated Thermosphere Ionosphere Demonstration System (Navy-HITIDES): Purpose, Design and Use

1. Executive Summary

The Earth's ionosphere is of significant importance for medium- and long-range high frequency (HF) communication, transionospheric communication, geolocation, and Over-The-Horizon Radar (OTHR) systems. Considering the worldwide application of OTHR, new capabilities to understand, model and predict the ionosphere globally translate directly into strategic and tactical battlefield advantages for the Navy. The Sun is the primary source of ionization of Earth's ionosphere that extends from the upper mesosphere (~70 km) through the thermosphere and into the exosphere (c.f. Figure 1). However, it is now recognized that meteorological influences propagating upward from the lower and middle atmosphere, including the troposphere and stratosphere, constitute a prominent contributor to unexplained day-to-day variability in the thermosphere/ionosphere region. Development of a skillful specification and prediction model of the ionosphere requires not only knowledge of the solar radiation and plasma outflow that reaches Earth, and the physics and chemistry of the thermosphere/ionosphere, but also an understanding of the role of the lower and middle atmosphere.

To achieve our goal to quantify the role of lower atmosphere weather for ionospheric variability, we have developed an atmosphere/ionosphere modeling capability that couples NRL's state-of-the-art physics-based ionosphere model, SAMI3 (Sami3 is Another Model of the Ionosphere), with the extended Whole Atmosphere Community Climate Model (WACCM-X). SAMI3, along with the coupling framework to the external thermosphere model, is called the Navy Highly Integrated Thermosphere Ionosphere Demonstration System (Navy-HITIDES). The ionospheric specifications produced by Navy-HITIDES/WACCM-X have been used to investigate day-to-day variability of the ionosphere during a stratospheric warming event (*McDonald et al*., 2015; *McDonald et al*., 2018) and the effects of lower atmospheric weather on thermospheric composition (*Sassi et al*., 2016).

This report describes the technical approach and implementation of atmosphere/ionosphere coupling in Navy-HITIDES. The document has a dual use: it is intended to be a general reference for users of Navy-HITIDES, while also providing documentation of the strategy used in order to achieve the final product.

This page intentionally left blank.

2. Background and Motivation

The direct effect of solar irradiance through photoionization is the primary driver of the generation of the ionosphere and its variability, however the majority of ionospheric plasma, which lies within the much denser thermosphere (95 – 500 km in altitude), is also influenced by variations in thermospheric composition, temperature and winds. Variations are generated predominantly by solar thermal tides arising from UV and EUV heating of the thermosphere, as well as high-latitude geomagnetic heating and momentum sources. Energy from the lower atmosphere also contributes, such as heating associated with absorption of solar radiation by water vapor (H_2O) in the troposphere and by ozone (O_3) in the stratosphere, which can generate upward propagating tides reaching the lower thermosphere.

It has been known for some time that the lower atmospheric contribution to variations in the thermosphere has a profound influence on the ionosphere. For example, day-to-day and longitudinal variability of the ionosphere not associated with geomagnetic activity has been attributed to processes originating in the lower atmosphere, including solar tides, planetary and gravity waves, and even infrasound (*Forbes and Garret*, 1979; *Killeen and Johnson*, 1995; *Forbes and Zhang*, 1997; *Hocke and Schlegel*, 1996; *Laštovička*, 2006). Although basic research still continues (e.g., *Forbes et al.,*, 2000; *Mendillo et al.,* 2002), only recently have we begun to understand specific mechanisms connecting the lower atmosphere to the ionosphere; it is now recognized that upward-propagating tides, planetary waves and gravity waves can couple into the ionosphere through modification of thermospheric composition, influences on *E* region conductivities, modulation of thermospheric temperature and wind structure, and generation of electric fields through dynamo action.

Navy-HITIDES coupled with WACCM-X has been developed with the objective to quantify the variability of the coupled thermosphere-ionosphere system that is associated with lower atmosphere weather when other drivers, such as the amount of solar electromagnetic radiation and geomagnetic parameters, are also included in simulations of the coupled system. Specific research questions that are being addressed with the coupled model include:

1. How does the ion composition affect radio-wave propagation?
2. What is the role of atmospheric waves that propagate from the lower atmosphere?
3. What level of environmental phenomena needs to be considered for next generation atmospheric radio-wave propagation models?

The coupling of Navy-HITIDES with WACCM-X presented two main technical challenges. The first challenge is that the ionosphere and atmosphere models utilize very different grid structures. While the ionosphere and thermosphere are components of the same region of the atmosphere, the fact that the ionospheric plasma is strongly coupled to the Earth's magnetic field is a complicating factor in developing a fully coupled ionosphere/thermosphere model. To properly account for the motion of the plasma, it is necessary to include its motion along the field lines, which extend tens of thousands of kilometers above Earth's surface. To this end, physics-based ionosphere models are

Manuscript approved January 23, 2019.

typically described in magnetic coordinates in order to simplify the equations to be solved. The thermosphere, on the other hand, is typically described on a pressure grid that extends to the exobase (~500 km). Thus, coupling the two grids requires robust interpolation routines, as well as a means to extend the thermospheric parameters into the exosphere to encompass the region of space mapped out by the SAMI3 geomagnetic field lines. The second technical challenge is that the coupled system must be computationally efficient. SAMI3 uses a semi-implicit scheme with a split adjustable time-step, which means that the time step is on the order of seconds in order to satisfy the Courant condition (see Section 4 of *Huba et al.*, 2000 for additional details). It was important to design Navy-HITIDES to run efficiently when coupled with WACCM-X so that months-long simulations could be completed within a reasonable amount of time.

Section 3 of this report provides a detailed description of Navy-HITIDES and the solutions to the technical challenges of coupling the model to WACCM-X. We also provide information on the important inputs/outputs of the model and instructions for running simulations. Section 4 briefly describes simulation results and examples of applications of the model. In Section 5, we summarize our conclusions and briefly describe future work. Several appendices provide additional details about Navy-HITIDES.

3. Model Description

The development of Navy-HITIDES necessitated an integration strategy that allows an efficient and accurate coupling of the neutral atmosphere physics with the ionosphere. In this section, we first describe each of the modeling components that comprise this effort (shown in Figure 2) and then describe in more detail how these components are coupled in order to provide a self-consistent simulation of the whole atmosphere and ionosphere.

As schematically illustrated in Figure 2, there are three crucial software components: an ionospheric model (SAMI3) that includes the physics of ion formation and transport; a neutral atmosphere model (WACCM-X) from ground to the exobase capable of informing the ionosphere on the weather of the day via atmospheric specifications (NAVGEM-HA); and a ray tracing code (MoJo) that is capable of using the ionospheric specifications to trace HF radio waves globally.

3a. SAMI3

SAMI3 (Sami3 is Another Model of the Ionosphere) is a comprehensive, physics-based, global model of the ionosphere developed at NRL. SAMI3 is based on SAMI2 (*Huba et al.*, 2000), a two-dimensional model of the ionosphere. SAMI3 models the plasma and chemical evolution of seven ion species (H^+, He^+, N^+, O^+, $N2^+$, NO^+ and $O2^+$) in the altitude range extending from 70 km to ~8 Re (Earth radii) and magnetic latitudes up to ±88°. Unique among ionospheric models, SAMI3 solves the ion continuity and momentum equations for all seven of the ion species, and solves the complete temperature equations for the electrons and three ion species (H^+, He^+ and O^+). Ion inertia is included in the ion momentum equation for motion along the geomagnetic field. SAMI3 is the only global ionosphere code that models full plasma transport for all of these ion species, including the molecular ions.

SAMI3 uses a fixed, non-uniform grid defined in the magnetic coordinate system. One axis of the grid is aligned with the Earth's geomagnetic field, allowing the model to distinguish between motion along the magnetic field and perpendicular to the magnetic field. The other two grid axes define magnetic east and a direction perpendicular to the magnetic field lines in the radial direction. Earlier versions of SAMI3 used a tilted dipole model of the earth's geomagnetic field. In the development of Navy-HITIDES, SAMI3 has been upgraded to allow the user to choose between a simple tilted dipole field or Magnetic Apex coordinates (*Richmond*, 1995), which includes a more accurate representation of the Earth's geomagnetic field, namely the International Geomagnetic Reference Field (IGRF).

Electric fields are solved self-consistently by solving a two-dimensional electrostatic potential equation that is derived from current conservation ($\nabla \cdot \mathbf{J} = 0$) in magnetic (currently magnetic-dipole) coordinates, and including gravity-driven currents. The perpendicular electric field is used in SAMI3 to calculate the mid- and low-latitude $\mathbf{E} \times \mathbf{B}$ drifts (*Huba et al*., 2008; 2010). The high-latitude region is electrodynamically coupled to the magnetosphere as a result of the interaction of the magnetized solar wind with Earth's geomagnetic field. To account for ion motion in the polar region, we have included a high-latitude electric potential from the Weimer-2005 model (*Weimer*, 2005). This is an empirical model that calculates how the polar electric potential responds to changes in the solar wind and interplanetary magnetic field (IMF). Details of the implementation of this model can be found in Appendix A.

Solar extreme ultraviolet (EUV) irradiances are specified using either the NRL Solar Spectral Irradiance (NRLSSI) model (*Lean et al.,* 2010) or using the EUV flux model for Aeronomic Calculations (EUVAC; *Richards et al.,* 1994). In its standard configuration, SAMI3 uses NRL Mass Spectrometer Incoherent Scatter (MSIS) climatology (*Picone et al*., 2003) to specify thermospheric composition and neutral temperature, and the Horizontal Wind Model (HWM14) (*Drob et al*., 2015) to specify the zonal and meridional thermospheric winds.

3b. WACCM-X

The Whole Atmosphere Community Climate Model, extended version (WACCM-X) is a global atmosphere model originally developed at the National Center for Atmospheric Research (NCAR). WACCM-X is built on WACCM, and can be accessed as a build option of the Community Earth System Model (CESM) numerical framework. WACCM interactively solves the global dynamics, physics and chemistry, from the ground to the model lid (see below). The chemistry module is interactive with the dynamics through transport and exothermic heating (*Kinnison et al*., 2007); photochemistry associated with major ion species (O^+, NO^+, O_2^+, N_2^+ and N^+) is part of the chemistry package. Photolysis rates are wavelength-dependent (*Woods and Rottman*, 2002; *Fröhlich* 2000; *Solomon and Qian*, 2005). The radiative heating calculation in WACCM is described in *Marsh et al*. (2007) and has the ability to parameterize the wavelength-dependent solar flux either in terms of the solar 10.7 cm radio flux (F10.7), or using NRL Solar Spectral Irradiances (NRLSSI; *Lean et al*., 2010). WACCM-X extends the atmosphere model into the thermosphere with the inclusion of additional thermospheric physics and electrodynamics interactions (*Liu et al*., 2010; *Liu et al*., 2018), including species-dependent specific heat and gas constant, major species diffusion, ion drag and frictional electron heating.

WACCM-X uses a geographic grid with uniform spacing in latitude and longitude, and a variable vertical resolution that is defined in terms of the local scale height. In its basic configuration, WACCM-X has 125 to 145 vertical levels from the ground to 4×10^{-10} hPa (500 to 700 km geometric height). The default vertical resolution is identical to WACCM below 0.96 hPa (see *Garcia et al*., 2007), and equal to ¼ scale height above that pressure level. The horizontal resolution is 1.9° x 2.5° (latitude x longitude) globally.

3c. Navy High-Altitude Atmospheric Specifications

In WACCM (and WACCM-X), specific events can be simulated by constraining the model meteorology with data analysis products or observations, using specified sea surface temperature at the lower boundary, and reconstructed spectral irradiances for the historical periods. The initial concepts and results from this model configuration, which is known as the specified dynamics WACCM (SD-WACCM), can be found in *Marsh* (2011).

Atmospheric specifications produced by the Navy Operational Global Atmospheric Prediction System – Advanced Level Physics High Altitude (NOGAPS-ALPHA) have been used to constrain (or nudge) the meteorology of WACCM-X (*Sassi et al.*, 2013). NOGAPS-ALPHA atmospheric analyses were produced using the 3DVAR NRL Atmospheric Validation Data Assimilation System (NAVDAS) and included observations from the ground throughout the middle atmosphere, extending the validity of the atmospheric fields up to 92 km. For more details, see *Hoppel et al*. (2008) and *Eckermann et al*. (2009).

The NOGAPS-ALPHA system was retired in 2012 and replaced by the prototype Navy Global Environmental Model High Altitude (NAVGEM-HA). NAVGEM-HA uses a hybrid 4DVAR data assimilation system (*Kuhl et al*., 2013) to ingest observations from the ground to about 100 km and, in combination with an 80-member ensemble of 6-hour forecasts that modify the static background error covariances, generates global 3-hourly synoptic analyses of key atmospheric variables (e.g., winds, temperatures, and constituents). The NAVGEM-HA system is fully described by *McCormack et al*. (2017), *Eckermann et al.* (2018), and references therein.

3d. MoJo

The MoJo (Modernized Jones) ray trace code calculates the ionospheric propagation path and observable properties of High Frequency (HF) radio waves. It is a modern, full physics 3-D High Frequency (HF) ray trace code. MoJo integrates the full Haselgrove equations (*Haselgrove and Haselgrove*, 1960) using one of three basic dispersion relationships including the gradients in all three directions of the local electron density, magnetic field components, and electron collision frequency. The implementation combines classical algorithms from the original Jones-Stephenson ray trace code (*Jones and Stephenson*, 1975) with modern programming techniques, resulting in an efficient computational engine. It should be noted that MoJo is actually not a stand-alone application, but rather an HF ray tracing toolbox written in Fortran 90 with

MATLAB® and Python® interfaces for developing customizable high-level end-user level applications.

MoJo computes propagation characteristics such as group delay, group path length, arrival angles, and deviative- and non-deviative absorption given an ionospheric specification, transmitter location, frequency, polarization mode, and initial propagation direction (e.g. *Zawdie et al.,* 2016; 2017). MoJo can provide these characteristics given a sufficiently accurate specification of the ionosphere, which can be used to meet the Navy requirements SR&T objectives put forth in SECNAVINST 2400.2A – "*DoD/Navy long-term needs of the environmental prediction of space weather effects for tactical planning purposes, as well as the maximization of systems performance though adaption to the variable environment"*.

3e. Navy-HITIDES Integration Scheme

With Navy-HITIDES, we have created a two-way coupling interface between WACCM-X and SAMI3. As shown in Figure 2, Navy-HITIDES consists of SAMI3 along with algorithms to exchange ion and neutral state variables with WACCM-X, interpolate quantities to and from the native grid of each model, and extend the neutral state variables above the altitude limit of WACCM-X.

In order to create the fully coupled ionosphere-thermosphere model, Navy-HITIDES has been implemented as a sub-component of the WACCM-X atmosphere component. In this configuration, the atmosphere and ionosphere are sequential instances of one prediction suite in which the cycling of the atmospheric model dictates the timing of the ionospheric simulation. An obvious disadvantage to this configuration is that the performance of the coupled system is constrained by the limitations of the slowest sub-component. In addition, the ionosphere sub-component must share the computational resources of the atmosphere component. Ideally, the ionosphere would be developed as a separate component, allowing Navy-HITIDES to have its own time management and runtime resource allocations. However, the WACCM atmospheric framework is designed to couple models that exchange surface or 2-dimensional geophysical fields; it becomes highly inefficient if 3-dimensional fields must be exchanged, as is the case with atmosphere-ionosphere coupling.

As mentioned in Section 2, the atmosphere in WACCM-X and the ionosphere in Navy-HITIDES employ vastly different grids such that information exchanged between the models must be interpolated at each time step (details in Section 3f). Rather than develop our own interpolation routines, we opted to use the software libraries provided with the Earth System Modeling Framework (ESMF). The advantage of ESMF is that it is tested, optimized and widely used across DoD, NASA and NSF applications. ESMF has also been adopted by the National Unified Operational Capability (NUOPC) which broadly describes an "Earth system prediction suite" that provides a common framework to facilitate the integration of models with different physics (*Theurich et al*., 2016). While we are using only the low-level interpolation routines in Navy-HITIDES, we note that CESM also has the capability to use ESMF time management services.

3f. Interpolation and Extension of Neutral Atmosphere Properties

The complexity of the problem of interpolating between a geographical and a geomagnetic grid is illustrated by Figure 3. The top left panel shows the WACCM-X grid: vertical levels are isobaric in the upper atmosphere, where the geopotential altitude of each grid point is determined hydrostatically; on each pressure level, the points are arranged in a regular and uniform latitude by longitude grid with a resolution of 1.9 by 2.5 degrees, respectively. The SAMI3 grid (top right panel in Figure 3) is instead arranged along the Earth's magnetic field lines with a fixed number of points along each field line. As shown in the horizontal plane (bottom right, Figure 3), the SAMI3 field lines are not coincident with the geographical longitudes. Because there is no particular correlation between WACCM-X and SAMI3 grid points, a very general interpolation capability is required. Generally, the problem illustrated by Figure 3 can be solved using a bilinear interpolation.

Bilinear interpolation requires the calculation of global weights to evaluate a field between the source grid and the target grid. The interpolation algorithm is simply

$$\Upsilon^k = \sum_{i=1}^{N} \mathrm{X}_i^k w_i \tag{1}$$

where Υ^k is the value at a point in the target grid, X_i^k are the values in the source grid that surround the target point, and w_i are the corresponding weights. For three dimensional interpolation N=8, meaning 8 weights are used in Eq. (1). The weights are calculated as the fractional distance between points in the source grid and a point of the target grid. The calculation of Υ^k according to Eq. (1) is relatively fast but the calculation of the 8 weights (which depends upon the calculation of the relative distances between all points in the grid) is expensive and therefore slow. Due to the fact that the location in altitude of the neutral atmosphere vertical levels changes every time step, the weights would need to be recalculated for every time step, making the evaluation of Eq. (1) untenable for practical applications. The solution we adopted is to introduce an intermediate grid.

Figure 4 describes the methodology implemented in Navy-HITIDES. Given the grid of the neutral atmosphere model (top left in Figure 4), we define an intermediate grid that is identical to that of the neutral atmosphere in the horizontal plane (i.e., same longitude and latitude points) but that has a finer and fixed resolution in the vertical dimension (top right in Figure 4); this grid is defined at the beginning of the simulation and does not change. We then calculate the ESMF weights to interpolate between the static neutral atmosphere intermediate grid and the ionospheric grid (bottom in Figure 4) at the beginning of the simulation, and we store the weights in memory. At each time step, when the pressure-level grid changes the altitude location of each neutral atmosphere grid point, Navy-HITIDES needs only to do a one-dimensional interpolation between the neutral atmosphere grid and the intermediate grid in each geographical column, followed by Eq. (1).

The interpolation described above only provides values of the neutral fields in the ionospheric domain up to the lid of the neutral atmosphere model (~ 500 km; the exobase); the neutral fields in the ionosphere above this altitude remain undetermined.

While there are theoretical formulations of the behavior of neutral fields above the exobase that allow for simple analytical extensions (*Bates,* 1959), the vertical extension of neutral fields in the model is complicated by the layout of the ionospheric grid; as noted above and shown in Figure 4, the ionospheric grid points are not aligned in geographical vertical columns, but rather follow geomagnetic field lines. This makes the vertical extension above the exobase significantly more complex. Our solution is to take a spherical harmonic decomposition of the neutral fields at a neutral atmosphere model (WACCM-X) level z_0 that is suitably near the lid and then apply the analytical extension using the Bates formulation on the SAMI3 grid at all altitudes above the WACCM-X lid. In the case of temperature T, for example:

$$T(\lambda, \theta) = \sum_{n=0}^{N} \sum_{m=-n}^{+n} T_{mn} Y_{mn}(\lambda, \theta) \tag{2}$$

where T is the temperature at a suitable level near the WACCM-X lid; T_{mn} are the coefficients of the spherical harmonics Y_{mn}; n and m are the global and longitudinal wavenumbers, respectively; and, λ and θ are the longitude and latitude, respectively. Equation (2) is inverted to obtain the coefficients T_{mn} using the algorithm developed by *Drob et al.* (2003). Once the coefficients T_{mn} are known, the vertical extension above the neutral atmosphere lid uses the Bates (1959) formulation. For temperature:

$$T(z) = T_{ex} - (T_{ex} - T_0)e^{-\sigma(z-z_0)} \tag{3 − 1}$$

where T_{ex} is the exospheric temperature, T_0 is the temperature at the reference level z_0, and

$$\sigma = \frac{\left(\frac{\partial T}{\partial z}\right)\Big|_{z_0}}{T_{ex} - T_0} \tag{3 − 2}$$

where the numerator is the vertical gradient of temperature at the reference level. For a constituent with concentration n:

$$n(z) = n_0 \left[\frac{T_0}{T(z)}\right]^{1+\gamma} e^{-\sigma\gamma(z-z_0)} \tag{3 − 3}$$

where

$$\gamma = \frac{mg}{\sigma k_B T_{ex}} \tag{3 − 4}$$

where m is the molecular mass of the constituent, g is the acceleration due to gravity (assumed spatially uniform, g=9.81 m/s^2), and k_B is the Boltzmann constant. Together, Eqs. (2) and (3) allow the calculation of temperature and constituents at any altitude above the neutral atmosphere model lid. For the neutral winds, the vertical extension only requires a spherical harmonic decomposition, as the winds are assumed to be uniformly constant at all altitudes above the reference level z_0. We note an important consequence of Eq. (2): the spectral resolution of the neutral field is determined by the native neutral atmosphere grid, but the reconstructed fields above the exobase have a spectral resolution dictated by the ionospheric grid. This can lead to incongruous behavior of the field across the z_0 interface, as we discuss below.

A simpler case occurs if $T_0 \approx T_{ex}$, that is, if the reference level is in the middle or upper thermosphere where the temperatures approximate the exospheric temperature. Then Eqs. (3-1) and (3-3) become

$$T(z) \approx T_{ex} \tag{4-1}$$

$$n(z) = n_0 e^{-(z-z_0)/H_{ex}} \tag{4-2}$$

where

$$\frac{1}{H_{ex}} = \frac{mg}{k_B T_{ex}} \tag{4-3}$$

Eqs (4-1,2) imply that if the extension is calculated from a level where the temperature is nearly identical to the exospheric value, temperatures at all altitudes above are uniform and equal to the exospheric value, and the constituent concentration is simply an exponential decay following the local scale height[1] (4-3). For practical application, Navy-HITIDES always assumes that the thermospheric fields are provided at an altitude where (4-1) is valid; then, (4-2) is used for the neutral composition and the neutral winds are extended uniformly constant at all altitudes.

Finally, as the vertical extension provides a fast and reasonable method to evaluate the neutral fields at all altitudes above the reference level, the extended fields are C^0 continuous in altitude if, and only if, the grid of the domain above the reference altitude z_0 (where spectral reconstruction [Eq. 2] and analytical extension [Eq. 3] take place) has the same horizontal resolution as the grid below z_0 (where interpolation [Eq. 1] operates). For Navy-HITIDES the SAMI3 grid is coarser in the longitudinal dimension than the WACCM-X grid, resulting in spectral truncation of the neutral fields when extended via (Eq. 2) and (Eq. 3); spectral truncation results in the extended fields not being C^0 continuous at the z_0 border. In order to mitigate this problem, the neutral fields that are used for the interpolation step (Eq. 1) are first spectrally filtered to an equivalent SAMI3 longitudinal resolution, making the resolution above and below z_0 congruous. Figure 5 summarizes the re-gridding and extension algorithms for these quantities; Figure 6 illustrates the results of the implementation of these algorithms in Navy-HITIDES, for two longitudinal slices showing (logarithm of) atomic oxygen and the zonal winds. It should be borne in mind that the geomagnetic field lines do not align with the geographic longitude (Figure 3); thus, the ionospheric longitudinal slices in Figure 6 are chosen to be the closest to the geographic longitudes of the accompanying WACCM-X panels.

[1] For improved accuracy, in actual implementation of the code, the scale height is calculated from the vertical derivative of the constituent. Eq. (4-3) is used only in the occasional circumstance when the numerical derivative produces un-physical results (e.g., negative H_{ex}).

3g. Interpolation of Ionospheric Properties

The second part of the two-way coupling between neutral atmosphere and ionosphere requires the return of ion velocities and density to the neutral atmosphere model. As mentioned in Section 3a, the SAMI3 grid is aligned with Earth's magnetic field, such that the three coordinate system component directions are 1) magnetic east; 2) along the magnetic field lines towards magnetic north; and 3) a direction that is perpendicular to the magnetic field lines in the radial direction. The ion velocities calculated by the SAMI3 model are therefore defined in these directions; in order to be returned to the neutral model, the ion velocities must first be projected into the geographic coordinate system, to provide values specifying velocity components in the geographic East, North and vertical directions. This step is accomplished through simple matrix multiplication, with details described in Appendix B.

Once the SAMI3 ion velocities have been converted to vectors in the geographic coordinate system, they must still be interpolated from the ionosphere grid to the neutral atmosphere geographic grid, along with the ion density. This proceeds as the inverse of the process shown in Figure 4: ESMF weights are used as indicated in Eq. (1) to interpolate from the SAMI3 grid to the intermediate grid, and then a one-dimensional interpolation is performed between the intermediate grid and the neutral atmosphere grid in each geographical column. For returning ionospheric quantities to the neutral atmosphere model neither spectral filtering nor a vertical extension as described in Section 3f are needed, however there is an issue with low altitudes. The bottom of the ionosphere grid is at ~80 km, while the neutral atmosphere grid extends essentially to the Earth's surface. Although ionospheric quantities should not be needed at low altitudes, to avoid potential numerical issues values are provided at all altitudes of the neutral atmosphere grid by extending the ionospheric quantities downwards in altitude with constant value. This is done using the geographic columns of the neutral atmosphere grid, so unlike the neutral atmosphere vertical extension spherical harmonic decompositions are not needed. Finally, due to the fact that the SAMI3 grid extends to ±88° magnetic latitude, but does not encompass the magnetic poles, after interpolation to the geographic grid there are small areas of missing value around the region of the magnetic poles. A simple one-dimensional interpolation in geographic longitude is used to provide values for these small regions.

3h. Navy-HITIDES Workflow

It should be noted that the Navy-HITIDES interface is designed to also operate as a stand-alone separate software component in which the ionosphere is executed offline and there is no effect of ionospheric physics on the thermosphere. The two configurations use the same interpolation algorithms and same baseline SAMI3 code, with only minor modifications; for example, solar parameters are obtained from WACCM-X in the integrated version vs. read from an external file in the standalone version, and simulation day, time and restart status are obtained from WACCM-X in the integrated version vs. read from namelist input in the standalone version.

A typical workflow for Navy-HITIDES, two-way coupled with WACCM-X is:

1. If at the beginning of the simulation, define the intermediate grid and calculate the ESMF weights.

2. Obtain neutral atmosphere fields at time $t_0+\Delta t$ from WACCM-X.
3. Perform spectral filtering of the neutral fields to the equivalent SAMI3 grid resolution.
4. Interpolate neutral fields to the static, intermediate grid via one-dimensional vertical interpolation.
5. Interpolate neutral fields from the intermediate grid to the ionospheric grid using ESMF weights.
6. Calculate vertical extension of the neutral fields above the WACCM-X lid using analytical formulations.
7. Solve for the ionospheric state between time t_0 and $t_0+\Delta t$.
8. Rotate ion velocities from magnetic coordinate directions to geographic coordinate directions.
9. Interpolate ion densities and velocities from the ionospheric grid to the intermediate grid using ESMF weights.
10. Interpolate ionospheric fields from the intermediate grid to the WACCM-X grid via one-dimensional vertical interpolation.
11. Calculate low altitude extension using uniform values to provide ionospheric fields below the bottom of the ionospheric grid.
12. Fill in ionospheric fields poleward of ±88 degrees magnetic latitude with a one-dimensional interpolation in geographic longitude.
13. Provide ionospheric fields at time $t_0+\Delta t$ to WACCM-X.

When integrated in the atmospheric model, the Navy-HITIDES model is invoked at the end of the dynamics step where full 3-dimensional fields of dynamics, energetics and composition are available. The resultant ionospheric state is provided to the atmospheric model via internal buffers. When Navy-HITIDES is run stand-alone, the atmospheric fields are expected to be available from an external file. In this case, the same workflow described above is used, except that the workflow truncates at step 7.

3i. Running Navy-HITIDES

Navy-HITIDES requires the following code dependencies:

- ESMF: https://www.earthsystemcog.org/projects/esmf/download/; any version greater than 7.0.0 is expected to work in Navy-HITIDES.
- NetCDF: https://www.unidata.ucar.edu/downloads/netcdf/index.jsp; version v4 or greater.
- MPI version v2. Different MPI implementations have been tested and work with Navy-HITIDES: Open MPI, MPICH, and Intel MPI.

The Navy-HITIDES code uses standard Message Passing Interface (MPI) protocol to work efficiently in modern distributed memory systems. Navy-HITIDES is MPI compliant and the results of its numerical simulations do not change with the number of MPI tasks requested. The code can run on an arbitrary number of processors, and will automatically attempt to define a SAMI3 grid distribution that divides longitude slices and field lines evenly across processors. When using the potential solver the maximum number of processors for reasonable model cost is ~96. Using fewer processors will increase wall-clock time, but decrease model cost. For maximum efficiency users should also take into account the number of processors per node on the available compute system when determining the ideal number of processors.

Details on the input configuration file (namelist input) for two-way coupled Navy-HITIDES are provided in Appendix C; details on the input configuration file for stand-alone Navy-HITIDES are provided in Appendix D. Appendix E provides the file naming and content convention that we have adopted for output. Model output is contained in NetCDF history files, with naming convention sami3_f*n*_*YYYYDDD*.nc, where *n* is an integer between 1 and 3, *YYYY* is the simulation year, and *DDD* is the simulation day, specified as day of year. Output cadence is user configurable through namelist file sami3_hitides_config.nml for the integrated code or namelist file sami3_config.nml for the stand-alone code; see Appendices C and D. Output fields are fully user configurable through namelist file sami3_nc_output.nml; see Appendix E for more information.

Informational messages, warnings, and model error messages are written to standard output. When Navy-HITIDES is integrated with WACCM-X this output is directed to log files with standard CESM naming conventions. When using the stand-alone code this output may be redirected to a file of the user's choice. Upon successful completion the model outputs the message "Model Completed Successfully!". In a typical batch system run-time errors and system level messages will appear in the batch system standard error and standard output files.

4. Applications

As illustrated above, Navy-HITIDES has been developed to investigate the physics of the coupling between the thermosphere and the ionosphere in the presence of day-to-day variations from the weather. Here we present some applications of Navy-HITIDES that address the goals outlined in Section 2.

4a. Ionospheric Variability

Figure 7 illustrates the effects of lower atmospheric weather on the ionosphere. It shows the peak electron density (NmF2) simulated by Navy-HITIDES with three different thermospheric drivers: a climatological thermosphere (top), a thermosphere coupled to WACCM-X that is nudged by atmospheric specifications generated by NOGAPS-ALPHA (middle), and a thermosphere coupled to WACCM-X but nudged by atmospheric specifications generated by NAVGEM-HA (bottom). Notice that the climatological thermosphere yields very little longitudinal structure, whereas the simulations using NOGAPS-ALPHA and NAVGEM-HA atmospheric specifications in the lower atmosphere show considerable ionospheric structure resembling observations (*Burns et al*., 2012)**.**

Figure 8 illustrates the relative importance of composition and winds on TEC at low latitudes. The top panel shows the total electron content (TEC) from a Navy-HITIDES simulation driven by winds and composition from a WACCM-X simulation that is nudged by NAVGEM-HA atmospheric specifications for January 2016. The bottom row shows sensitivity simulations in which the thermospheric winds (left panel) or the composition (right panel) are replaced independently with climatology. These sensitivity experiments clearly illustrate that at low latitudes the neutral winds are the major drivers of the TEC variability, while day-to-day variability of composition has a secondary effect.

4b. HF Radio Wave Propagation

Figure 9 illustrates that the output from Navy-HITIDES may be used as the ionospheric specification for the simulation of HF radio wave propagation or ray-tracing. In this case, the NRL HF propagation code MoJo (Modernized Jones Code) was utilized to simulate the signal strength of 7 MHz radio waves over the pacific ocean. The radio waves are sensitive to the distribution and gradients in the ionospheric density, so the propagation paths and signal strength for a given location can change significantly depending on the conditions in the ionosphere. In this case, the signal strength is shown to change significantly due to the location of the day/night terminator. The signal is strongest close to the transmitter, which is on the day side of the terminator. The range of the signal is extended on the nightside due to decreased absorption. These simulations have the potential to predict the response of existing Navy radars to changing ionospheric conditions.

One example is the simulation of backscatter power from an Over-The-Horizon-Radar (OTHR). Figure 10 shows the simulated backscatter power as a function of time (over the course of five days) and virtual range. The top panel of Figure 10 shows the simulated backscatter power generated using a climatological ionosphere as the background for the ray-tracing calculation. Since the climatology does not represent the daily variations in the ionosphere, it is unable to reproduce daily changes in backscatter power. However, it is interesting that an echo is shown before sunrise, which is likely to be the result of reflection from the F-layer. The bottom panel of Figure 10 shows the simulated backscatter power generated using output from Navy-HITIDES driven by WACCM-X nudged by NAVGEM-HA. The ionospheric model driven by lower atmospheric weather is more similar to observations and predicts backscatter power variations from day to day.

5. Conclusion and Future Directions

This report describes the efforts undertaken by NRL scientists and contractors over a period of five years to create the first Navy ionosphere model, Navy-HITIDES, coupled to a whole atmosphere model. The goal of the project was to quantify the effects of atmospheric weather on the ionospheric structure and variability. The fulfillment of this goal can been seen in work such as *McDonald et al.* (2015), where we show that the day-to-day variability of total electron content (TEC) as determined by the non-migrating tides is in agreement with observations at about 16% of the mean peak value, while climatological models show no variability altogether. In *McDonald et al.* (2018) we show that in order to capture the effects of tides on the ionosphere with high fidelity, the required cadence of atmospheric behavior used to drive the whole atmosphere simulation must be at least 3 hours in order to fully resolve at least the semidiurnal migrating solar tide, which is a prominent driver of ionospheric changes and structure.

The product of this five year effort includes the physics of the SAMI3 model, optimized for efficient execution on modern massively parallel super-computers, and an interface that includes interpolation and extrapolation algorithms that facilitate the interactions between the ionosphere and a whole atmosphere model. Navy-HITIDES is based on an existing physics-based ionospheric model, and its interfaces are sufficiently general to be adapted to most whole atmosphere models that are available today. It should be borne in mind that Navy-HITIDES is a global model; the development of a regional capability is beyond the scope of this project and is left to future activities. The results shown from Navy-HITIDES simulations clearly demonstrate the importance of including atmospheric weather in ionospheric simulations, especially when forecasting of the ionospheric conditions is required. Thus, while Navy-HITIDES is a research product, future directions and applications for Navy operational forecasts can use this product to advance the integration of ionospheric and whole atmosphere models. A prominent outcome of this project is that the tools created under its aegis are without doubt useful for the development of a future operational Navy capability.

6. Acknowledgments. We thank the Whole Atmosphere Community Climate Model and the Community Earth System Model Working Groups at the *National Center for Atmospheric Research* (Boulder – CO) for useful conversations. We thank also the support from the ESMF group on the usability and implementation of ESMF libraries. This work was supported by the Chief of Naval Research.

Appendix A

Weimer-2005 is an empirical model (*Weimer*, 2005) that calculates how the polar electric potential responds to changes in the solar wind and interplanetary magnetic field (IMF); it is based on spherical harmonic fits to satellite measurements of the polar ionospheric electric field. The Weimer-2005 model requires as input the solar wind velocity and density at the magnetopause, the y- and z-components of the IMF at the magnetopause, and Earth's dipole tilt angle. Time-dependent data for the solar wind and the IMF can be obtained from the NASA/GSFC Space Physics Data Facility (SPDF) OMNIWeb service, where spacecraft data is available in 1-minute intervals. Prior to running Navy-HITIDES the appropriate solar wind and IMF data must be downloaded, time-averaged using a 20-minute averaging window, and written to NetCDF for use at run-time; the Navy-HITIDES distribution includes processing software to handle these tasks.

During Navy-HITIDES execution, the Weimer potential is calculated as a function of magnetic latitude and magnetic local time (MLT), where the latter is a proxy for magnetic longitude. The Weimer-2005 model only returns values in a region approximately north of 60° magnetic latitude; for magnetic latitudes south of this, the model returns a fill value, which is specified as zero. Since the model is derived from spherical harmonic fits to data on the surface of a sphere, it has no altitude dependence. In the Navy-HITIDES code an appropriate latitude grid for the Weimer model is derived by taking the magnetic latitude at the lowest altitude of the native SAMI3 grid for each field line; MLT is calculated for each SAMI3 magnetic longitude based on solar position. The Weimer potential is updated every time step to properly calculate the MLT dependence, however the input solar wind and IMF data are only updated every 15 model minutes. Since the SAMI3 magnetic field lines are equipotential surfaces, the Weimer potential for each field line is added to the dynamo electric potential, and the sum of the two potentials is used for calculating the ionospheric electric field and ion velocities. In general, inclusion of the Weimer high-latitude electric potential leads to larger ion velocities near the magnetic poles, as well as larger variations in ion and electric density at high latitudes.

Appendix B

As mentioned in Sections 3a and 3g, the three coordinate system component directions for the SAMI3 ionosphere system are: 1) magnetic east, labeled $\hat{\boldsymbol{h}}$; 2) magnetic north, labeled $\hat{\boldsymbol{s}}$; and 3) a direction that is perpendicular to the magnetic field lines in the radial direction, labeled $\hat{\boldsymbol{p}}$. For the geographic grid of the neutral atmosphere system the three coordinate system component directions are: 1) geographic east, labeled $\hat{\boldsymbol{\varphi}}$; 2) geographic north, labeled $\hat{\boldsymbol{\lambda}}$; and 3) vertical, labeled $\hat{\boldsymbol{r}}$. Since SAMI3 assumes the Earth is spherical $\hat{\boldsymbol{r}}$ is always radially outward. The relative orientation of the geomagnetic and geographic coordinate systems varies over the globe, such that the transformation matrices between the coordinate systems are dependent on location; this is illustrated in Figures 11 and 12. Figure 11 shows how $\hat{\boldsymbol{h}}$ and $\hat{\boldsymbol{s}}$ (rightward and upward red arrows, respectively) vary with the magnetic field lines (green lines on map), while $\hat{\boldsymbol{\varphi}}$ and $\hat{\boldsymbol{\lambda}}$ (rightward and upward blue lines, respectively) have a fixed geographic orientation. Note that $\hat{\boldsymbol{s}}$ also has a varying vertical orientation that cannot be seen in Figure 11. Figure 12 shows how the relative orientation between $\hat{\boldsymbol{s}}$ and $\hat{\boldsymbol{p}}$ (red arrows) and $\hat{\boldsymbol{\lambda}}$ and $\hat{\boldsymbol{r}}$ (blue arrows) varies along the magnetic field lines. At the magnetic equator $\hat{\boldsymbol{r}}$ and $\hat{\boldsymbol{p}}$ are essentially identical, but at the magnetic poles $\hat{\boldsymbol{r}}$ is instead aligned with $\hat{\boldsymbol{s}}$; the two are nearly parallel at the south magnetic pole and nearly antiparallel at the north magnetic pole. Note that Figure 12 shows field lines and unit vectors extending to an altitude of ~5000 km, but in the Navy-HITIDES model coupling the relative vector orientations are only relevant in the domain of the neutral atmosphere, up to ~500 km altitude.

The Navy-HITIDES code takes a strictly numerical approach to calculating the location dependent transformation matrices between the two coordinate systems. During initialization unit vectors describing both coordinate systems are numerically calculated in terms of Cartesian Earth Centered Earth Fixed (ECEF) coordinates at each SAMI3 grid point. The use of the ECEF coordinate system makes it possible to easily calculate dot products between geomagnetic and geographic vectors. The elements of the coordinate transformation matrices are then calculated as dot products between the unit vectors of the two coordinate systems. Specifically, to transform neutral winds from the neutral atmosphere coordinate system to the ionospheric coordinate system the following equations apply:

$$Vh_n = (\hat{\boldsymbol{\varphi}} \cdot \hat{\boldsymbol{h}})U_n + (\hat{\boldsymbol{\lambda}} \cdot \hat{\boldsymbol{h}})V_n + (\hat{\boldsymbol{r}} \cdot \hat{\boldsymbol{h}})W_n \qquad (5-1)$$

$$Vs_n = (\hat{\boldsymbol{\varphi}} \cdot \hat{\boldsymbol{s}})U_n + (\hat{\boldsymbol{\lambda}} \cdot \hat{\boldsymbol{s}})V_n + (\hat{\boldsymbol{r}} \cdot \hat{\boldsymbol{s}})W_n \qquad (5-2)$$

$$Vp_n = (\hat{\boldsymbol{\varphi}} \cdot \hat{\boldsymbol{p}})U_n + (\hat{\boldsymbol{\lambda}} \cdot \hat{\boldsymbol{p}})V_n + (\hat{\boldsymbol{r}} \cdot \hat{\boldsymbol{p}})W_n \qquad (5-3)$$

where Vh_n, Vs_n and Vp_n are the geomagnetic $\hat{\boldsymbol{h}}$, $\hat{\boldsymbol{s}}$ and $\hat{\boldsymbol{p}}$ components of the neutral wind, respectively, and U_n, V_n and W_n are the geographic zonal ($\hat{\boldsymbol{\varphi}}$), meridional ($\hat{\boldsymbol{\lambda}}$) and vertical ($\hat{\boldsymbol{r}}$) components of the neutral wind, respectively. These equations are used in the SAMI3 code regardless of whether the neutral winds are supplied by the WACCM-X neutral atmosphere model, or the analytic HWM14 model. The use of numeric dot products allows for seamless switching between dipole and Magnetic Apex coordinates for the ionosphere grid; although the actual definitions of $\widehat{\boldsymbol{h}}$, $\widehat{\boldsymbol{s}}$ and $\widehat{\boldsymbol{p}}$ in ECEF coordinates will change, Eqs (5-1,2,3) apply in either case.

The following equations are used in the Navy-HITIDES model for rotating the ion velocities from the ionospheric coordinate system to the neutral atmosphere coordinate system:

$$U_{ion} = (\widehat{\boldsymbol{\varphi}} \cdot \widehat{\boldsymbol{p}})Vp_{ion} + (\widehat{\boldsymbol{\varphi}} \cdot \widehat{\boldsymbol{h}})Vh_{ion} \quad (6-1)$$

$$V_{ion} = (\widehat{\boldsymbol{\lambda}} \cdot \widehat{\boldsymbol{p}})Vp_{ion} + (\widehat{\boldsymbol{\lambda}} \cdot \widehat{\boldsymbol{h}})Vh_{ion} \quad (6-2)$$

$$W_{ion} = (\widehat{\boldsymbol{r}} \cdot \widehat{\boldsymbol{p}})Vp_{ion} + (\widehat{\boldsymbol{r}} \cdot \widehat{\boldsymbol{h}})Vh_{ion} \quad (6-3)$$

where U_{ion}, V_{ion} and W_{ion} are the geographic zonal, meridional and vertical components of the ion velocity, respectively, and Vp_{ion} and Vh_{ion} are the geomagnetic $\widehat{\boldsymbol{p}}$ and $\widehat{\boldsymbol{h}}$ components of the ion velocity, respectively. In Eqs (6-1,2,3) the $\widehat{\boldsymbol{s}}$ component of the ion velocity has been neglected, because only **E** × **B** drifts, which are perpendicular to the magnetic field lines, are returned in the two-way coupling.

Appendix C

The following is an example of the sami3_hitides_config.nml file for use with two-way coupled Navy-HITIDES:

```
&RUNCONFIG
 USE_WACCM_WIND = .TRUE.
 USE_WACCM_NEUT = .TRUE.
 FEJER = .FALSE.
 APEX = .TRUE.
 DTHR = 900.0
 HRPR = 0.
 INPUT_DIR = '/home/jtate/sami_inputs'
 HIGH_LAT_MODEL = 'weimer'
 WEIMER_FILE = 'weimer_data_Jan2010.nc'
/
```

USE_WACCM_WIND – Set to .true. to use neutral winds input from WACCM-X; set to .false. to obtain neutral winds from the HWM14 model

USE_WACCM_NEUT – Set to .true. to use neutral temperature and composition input from WACCM-X; set to .false. to obtain neutral temperature and composition from the MSIS model

FEJER – Set to .true. to enable use of the analytic Scherliess-Fejer Drift model for calculating ion drift velocities; set to .false. to calculate drift velocities from the electric potential

APEX – Set to .true. to enable use of Magnetic Apex coordinates; set to .false. to use native SAMI3 magnetic dipole coordinates

DTHR – Output cadence in seconds; applies to all SAMI3 time-dependent NetCDF output files

HRPR – Number of model hours to run before writing output to time-dependent NetCDF output files; historically this input has been used to suppress output during the spin-up period, approximately the first 24 hours of a simulation

INPUT_DIR – Directory where all SAMI3 input files are located; directory reference may be absolute or relative to the run directory

HIGH_LAT_MODEL – Toggle switch for use of an external high-latitude potential model; current valid values are 'none' or 'weimer'

WEIMER_FILE – Name of input file for Weimer model data; only required if using Weimer high-latitude potential model

Appendix D

The following is an example of the sami3_config.nml file for use with stand-alone Navy-HITIDES; a commented version is included in the Navy-HITIDES distribution in the src/sami_hitides directory:

```
! Namelist input for SAMI3-HITIDES
&RUNCONFIG
 DAY = 1
 YEAR = 2010
 DTHR = 900.0
 HRPR = 0.
 HRINIT = 0.
 RUN_LENGTH = 86400.
 DAYBOUND = 24.
 FEJER = .FALSE.
 APEX = .TRUE.
 RESTART = .FALSE
 INPUT_DIR = '/home/jtate/sami_inputs'
 USE_WACCM_WIND = .TRUE.
 USE_WACCM_NEUT = .TRUE.
 WACCM_NC = 'f_waccmx_SD_NAVGEM_1hr_new.cam.h4'
 SOLARPARMS = 'WACCM'
 HIGH_LAT_MODEL = 'weimer'
 WEIMER_FILE = 'weimer_data_Jan2010.nc'
 START_LON = 0.
 DELLON = 360.
 BLAT_MAX = 88.
 IC_FILE = ‘ ‘
 FOURTH_ORDER_TRANSPORT = .FALSE.
/
```

DAY – Day of year to start or continue simulation

YEAR – Simulation year

DTHR – Output cadence in seconds; applies to all SAMI3 time-dependent NetCDF output files

HRPR – Number of model hours to run before writing output to time-dependent NetCDF output files; historically this input has been used to suppress output during the spin-up period, approximately the first 24 hours of a simulation

HRINIT – Simulation start time in decimal UT hours

RUN_LENGTH – Simulation run time in seconds

DAYBOUND – Sets the length of the first simulation day in hours; should always be set to 24.

FEJER – Set to .true. to enable use of the analytic Scherliess-Fejer Drift model for calculating ion drift velocities; set to .false. to calculate drift velocities from the electric potential

APEX – Set to .true. to enable use of Magnetic Apex coordinates; set to .false. to use native SAMI3 magnetic dipole coordinates

RESTART – Set to .false. to start a new simulation; set to .true. to continue an existing simulation, which requires the presence of a restart file specified by the DAY and YEAR input variables

INPUT_DIR – Directory where all SAMI3 input files are located; directory reference may be absolute or relative to the run directory

USE_WACCM_WIND – Set to .false. to obtain neutral winds from the HWM14 model; set to .true. to read neutral winds from a WACCM-X history file

USE_WACCM_NEUT – Set to .false. to obtain neutral temperature and composition from the MSIS model; set to .true. to read neutral temperature and composition from a WACCM-X history file

WACCM_NC – File stem for input WACCM-X file; may include a directory path; only required if either USE_WACCM_WIND or USE_WACCM_NEUT is set to .true.

SOLARPARMS – Toggle switch for type of solar parameter input (F10.7, F10.7a, and Ap); current valid values are 'WACCM' (recommended) or 'NRLEUV'

HIGH_LAT_MODEL – Toggle switch for use of an external high-latitude potential model; current valid values are 'none' or 'weimer'

WEIMER_FILE – Name of input file for Weimer model data; only required if using Weimer high-latitude potential model

START_LON – Only used for wedge grid (regional) simulations; specifies western edge of the grid in geographic longitude at the magnetic equator

DELLON – Activates wedge grid (regional) mode if value is less than 360; specifies width of the wedge in magnetic longitude

BLAT_MAX – Maximum magnetic latitude of the grid

IC_FILE – Name of initialization file for wedge grid simulations; if left blank, the code will attempt to initialize from a standard restart file

FOURTH_ORDER_TRANSPORT – Toggle switch to use 4th order transport code (still in testing)

Appendix E

NetCDF output from SAMI3 is configured using a NetCDF-specific namelist file, sami3_nc_output.nml, which is included in the Navy-HITIDES distribution in the src/sami_hitides directory.

NetCDF output from SAMI3 currently allows for four different files to be produced, hereafter referred to as F1 through F4. Files F1 through F3 allow for time-dependent output, with a naming convention that includes the year and day of the simulation, while F4 is used for static output related to the SAMI3 grid.

SAMI3 NetCDF Output File Descriptions		
F1	sami3_f1_*YYYYDDD*.nc	Any time-varying variable can appear in this file. This file is always produced, but contains only the SAMI3 grid in geographic coordinates if no time-varying fields have been requested.
F2	sami3_f2_*YYYYDDD*.nc	Any time-varying variable can appear in this file. This file is only produced if the user selects output fields for the file in the SAMI3 NetCDF namelist.
F3	sami3_f3_*YYYYDDD*.nc	Any time-varying variable can appear in this file. This file is only produced if the user selects output fields for the file in the SAMI3 NetCDF namelist.
F4	sami3_f4.nc	Static grid-related variables. This file is only produced if the user selects output fields for the file in the SAMI3 NetCDF namelist.

The NetCDF namelist file contains fields that allow the user to specify which quantities, if any, should appear in each of the four files. These settings are called FIELDS_OUT_F1, FIELDS_OUT_F2, FIELDS_OUT_F3, and FIELDS_OUT_F4; they should be set to a comma-separated list of quantities to be output into the relevant file. For files F2 through F4, if no output fields are requested in the namelist, the files are not produced. The following is an example of the sami3_nc_output.nml file:

```
&NCDATA
 FIELDS_OUT_F1 = 'dene', 'u1p', 'u3h'
 FIELDS_OUT_F2 = 'u1', 'u2'
 FIELDS_OUT_F3 = ‘ ‘
 FIELDS_OUT_F4 = 'blats', 'blons', 'balts'
/
```

This example indicates that the user does not wish file F3 to be produced, and wishes files F1, F2, and F4 to contain the listed output fields. The table below identifies the names of the fields which the user can place in the NetCDF namelist, a description of the physical quantity described by the field, and the file(s) in which the field can appear.

SAMI3 NetCDF Output Field Information					
Field Name	**F1**	**F2**	**F3**	**F4**	**Description**
dene	x	x	x		Electron density (cm-3)
deni1	x	x	x		Ion species #1 (H^+) density (cm-3)
deni2	x	x	x		Ion species #2 (O^+) density (cm-3)
deni3	x	x	x		Ion species #3 (NO^+) density (cm-3)
deni4	x	x	x		Ion species #4 ($O2^+$) density (cm-3)
deni5	x	x	x		Ion species #5 (He^+) density (cm-3)
deni6	x	x	x		Ion species #6 ($N2^+$) density (cm-3)
deni7	x	x	x		Ion species #7 (N^+) density (cm-3)
denn1	x	x	x		Neutral species #1 (H) density (cm-3)
denn2	x	x	x		Neutral species #2 (O) density (cm-3)
denn3	x	x	x		Neutral species #3 (NO) density (cm-3)
denn4	x	x	x		Neutral species #4 (O2) density (cm-3)
denn5	x	x	x		Neutral species #5 (He) density (cm-3)
denn6	x	x	x		Neutral species #6 (N2) density (cm-3)
denn7	x	x	x		Neutral species #7 (N) density (cm-3)
te	x	x	x		Electron temperature (K)
ti1	x	x	x		Ion temperature for species #1 (K)
ti2	x	x	x		Ion temperature for species #2 (K)
ti3	x	x	x		Ion temperature for species #3 (K)
ti4	x	x	x		Ion temperature for species #4 (K)
ti5	x	x	x		Ion temperature for species #5 (K)

ti6	x	x	x		Ion temperature for species #6 (K)
ti7	x	x	x		Ion temperature for species #7 (K)
vsi1	x	x	x		Ion velocity for species #1 (cm/s)
vsi2	x	x	x		Ion velocity for species #2 (cm/s)
vsi3	x	x	x		Ion velocity for species #3 (cm/s)
vsi4	x	x	x		Ion velocity for species #4 (cm/s)
vsi5	x	x	x		Ion velocity for species #5 (cm/s)
vsi6	x	x	x		Ion velocity for species #6 (cm/s)
vsi7	x	x	x		Ion velocity for species #7 (cm/s)
u1p	x	x	x		ExB drift velocity, p-direction (vexbp) (cm/s)
u2s	x	x	x		ExB drift velocity across s-face (vexbs) (cm/s)
u3h	x	x	x		ExB drift velocity, h-direction (vexbh) (cm/s)
u1	x	x	x		Zonal neutral wind (cm/s)
u2	x	x	x		Meridional neutral wind (cm/s)
u3	x	x	x		Vertical neutral wind (cm/s)
hipc	x	x	x		Field-line integrated Pedersen conductivity
hihc	x	x	x		Field-line integrated Hall conductivity
sigmap	x	x	x		Pedersen conductivity
sigmah	x	x	x		Hall conductivity
sigmapic	x	x	x		Ion Pedersen conductivity
sigmahic	x	x	x		Ion Hall conductivity
vnq	x	x	x		Neutral wind velocity in q-direction (cm/s)
vnp	x	x	x		Neutral wind velocity in p-direction (cm/s)
vnphi	x	x	x		Neutral wind velocity in phi-direction (cm/s)

hipcp	x	x	x		Field-line integrated value in potential equation
hipcphi	x	x	x		Field-line integrated value in potential equation
hihcm	x	x	x		Field-line integrated value in potential equation
hidpv	x	x	x		Field-line integrated value in potential equation
hidphiv	x	x	x		Field-line integrated value in potential equation
hidpg	x	x	x		Field-line integrated value in potential equation
hidphig	x	x	x		Field-line integrated value in potential equation
phi	x	x	x		Two-dimensional electric potential used to calculate ion velocities (statvolt)
phi_high_lat	x	x	x		High-latitude component of phi, imposed by an external model such as Weimer (statvolt)
zalt	x	x	x	x	Altitude - s-grid (km)
glat	x	x	x	x	Geographic latitude - s-grid
glon	x	x	x	x	Geographic longitude - s-grid
balts				x	Magnetic altitude - s-grid (km)
blats				x	Magnetic latitude - s-grid
blons				x	Magnetic longitude - s-grid
xs				x	x-coordinate s-grid (cm)
ys				x	y-coordinate s-grid (cm)
zs				x	z-coordinate s-grid (cm)
baltp				x	Magnetic altitude - p-grid (km)
blatp				x	Magnetic latitude - p-grid
blonp				x	Magnetic longitude - p-grid
xp				x	x-coordinate p-grid (cm)
yp				x	y-coordinate p-grid (cm)

zp				**x**	z-coordinate p-grid (cm)
vssnx				**x**	Unit vector in s-direction, x-component - s-grid
vssny				**x**	Unit vector in s-direction, y-component - s-grid
vssnz				**x**	Unit vector in s-direction, z-component - s-grid
vpsnx				**x**	Unit vector in p-direction, x-component - s-grid
vpsny				**x**	Unit vector in p-direction, y-component - s-grid
vpsnz				**x**	Unit vector in p-direction, z-component - s-grid
vhsnx				**x**	Unit vector in h-direction, x-component - s-grid
vhsny				**x**	Unit vector in h-direction, y-component - s-grid
vhsnz				**x**	Unit vector in h-direction, z-component - s-grid
gsphix				**x**	Unit vector in geographic longitude direction, x-component - s-grid
gsphiy				**x**	Unit vector in geographic longitude direction, y-component - s-grid
gsphiz				**x**	Unit vector in geographic longitude direction, z-component - s-grid
gsthetax				**x**	Unit vector in geographic latitude direction, x-component - s-grid
gsthetay				**x**	Unit vector in geographic latitude direction, y-component - s-grid
gsthetaz				**x**	Unit vector in geographic latitude direction, z-component - s-grid
gsrx				**x**	Unit vector in geographic altitude direction, x-component - s-grid
gsry				**x**	Unit vector in geographic altitude direction, y-component - s-grid
gsrz				**x**	Unit vector in geographic altitude direction, z-component - s-grid

References

Bates, D.R. (1959). Some problems concerning the terrestrial atmosphere above about the 100 km level. *Proc. R. Soc. London Ser. A 253*, 451–462, doi:10.1098/rspa.1959.0207.

Burns, A.G., S.C. Solomon, W. Wang, L. Qian, Y. Zhang, and L.J. Paxton (2012). Daytime climatology of ionospheric NmF2 and hmF2 from COSMIC data. *J. Geophys. Res.*, **117**, doi:10.1029/2012JA017529.

Drob, D.P., J.M. Picone, and M. Garces (2003). Global morphology of infrasound waves. *J. Geophys. Res.*, **108**, doi:10.1029/2002JD003307.

Drob, D.P. et al. (2015). An update to the Horizontal Wind Model (HWM): The quiet time thermosphere. *Earth and Space Science*, **2**, 301–319, doi:10.1002/2014EA000089.

Eckermann, S. D., K. W. Hoppel, L. Coy, J. P. McCormack, D. E. Siskind, K. Nielsen, A. Kochenash, M. H. Stevens, C. R. Englert, M. Hervig (2009). High-altitude data assimilation system experiments for the northern summer mesosphere season of 2007. *J. Atmos. Sol. Terr. Phys.*, **71**, 531–551.

Eckermann, S.D. et al. (2018). High-Altitude (0–100 km) Global Atmospheric Reanalysis System: Description and Application to the 2014 Austral Winter of the Deep Propagating Gravity Wave Experiment (DEEPWAVE). *Mon. Wea. Rev.*, **146**, 2639-2666, doi:10.1175/MWR-D-17-0386.1.

Forbes, J. M., & Garrett, H. B. (1979). Theoretical studies of atmospheric tides. *Reviews of Geophysics*, *17*(8), 1951–1981, doi:10.1029/RG017i008p01951.

Forbes, J.M., and X. Zhang (1997), Quasi 2-day oscillations of the ionosphere: A statistical study, *J. Atmos. Solar-Terr. Phys.*, *59*(9), 1025-1034.

Forbes, J.M., S.E. Palo, and X. Zhang (2000), Variability of the ionosphere, *J. Atmos. Solar-Terr. Phys.*, **62**, 685-693.

Fröhlich, C., 2000. Observations of irradiance variations. *Space Sci. Rev.*, **94**, 15-24.

Hoppel, K.W., N.L. Baker, L. Coy, S.D. Eckermann, J.P. McCormack, G.E. Nedoluha, and E. Siskind (2008). Assimilation of stratospheric and mesospheric temperatures from MLS and SABER into a global NWP model. *Atmos. Chem. Phys.*, **8**, 6103-6166.

Garcia, R.R., D.R. Marsh, D.E. Kinnison, B.A. Boville, F. Sassi (2007). Simulations of secular trends in the middle atmosphere, 1950-2003. *J. Geophys. Res.*, **112**, doi:10.1029/2006JD007485.

Haselgrove, C. B., and J. Haselgrove (1960). Twisted ray paths in the ionosphere, *Proc. Phys. Soc. London*, **75**, 357–363.

Hocke, K., and K. Schlegel (1996), A review of atmospheric gravity waves and traveling ionospheric disturbances: 1982 – 1995, *Ann. Geophys.*, *14*(9), 917-940.

Huba, J.D., G. Joyce, and J.A. Fedder (2000). Sami2 is Another Model of the Ionosphere (SAMI2): A new low-latitude ionosphere model. *J. Geophys. Res.*, **105**, 23,035-23,053.

Huba, J. D., G. Joyce, and J. Krall (2008), Three- dimensional equatorial spread F modeling, *Geophys. Res. Lett*., **35**, L10102, doi:10.1029/2008GL033509.

Huba, J.D., G. Joyce, J. Krall, C.L. Siefring, and P.A. Bernhardt (2010). Self-consistent modeling of equatorial dawn density depletions with SAMI3. *Geophys. Res. Lett.*, **37**, doi:10.1029/2009GL041492.

Jones, R.M. and J.J. Stephenson (1975). A versatile three-dimensional ray tracing computer program for radio waves in the ionosphere, *NASA STI/Recon Technical Report N*, **76**, 25,476.

Killeen, T. L., and R. M. Johnson (1995). Upper atmospheric waves, turbulence and winds: Importance for mesospheric and thermospheric studies. *Rev. Geophys.*, **33**, 737–744, doi:10.1029/95RG00408.

Kinnison, D.E. et al. (2007). Sensitivity of chemical tracers to meteorological parameters in the MOZART-3 chemical transport model. *J. Geophys. Res.*, **112**, doi:10.1029/2006JD007879.

Kuhl, D., T. Rosmond , C. Bishop, J. McLay, N. Baker (2013). Comparison of hybrid ensemble/4DVar and 4DVar within the NAVDAS-AR data assimilation framework. *Mon. Wea. Rev.*, **141**, 2740–2758.

Laštovička, J. (2006), Forcing of the ionosphere by waves from below, *J. Atmos. Solar-Terr. Phys.*, **68**, 479-497.

Lean, J. L., T. N. Woods, F. G. Eparvier, R. R. Meier, D. J. Strickland, J. T. Correira, and J. S. Evans, 2010. Solar Extreme Ultraviolet Irradiance: Present, Past and Future, *J. Geophys. Res*., doi:10.1029/2010JA015901.

Liu, H.-L., et al. (2010). Thermosphere extension of the Whole Atmosphere Community Climate Model (2010). *J. Geophys. Res.*, **115**, doi:10.1029/2010JA015586.

Liu, H.-L., et al. (2018). Development and validation of the Whole Atmosphere Community Climate Model with thermosphere and ionosphere extension (WACCM-X 2.0). *Journal of Advances in Modeling Earth Systems*, **10**, 381-402, https://doi.org/ 10.1002/2017MS001232.

Marsh, D.R., R.R. Garcia, D.E. Kinnison, B.A. Boville, F. Sassi, S.C. Solomon, and K. Matthes (2007). Modeling the whole atmosphere response to solar cycles changes in radiative and geomagnetic forcing. *J. of Geophys. Res.*, **112**, doi:10.1029/2006JD008306.

Marsh, D.R. (2011). Chemical-dynamical coupling in the mesosphere and lower thermosphere. In *Aeronomy of the Earth's Atmosphere and Ionosphere*. Eds.: Abdu M.A.; Pancheva D.; and, Bhattacharyya A. IAGA Special Sopron Book Series. Doi: 10.1007/978-94-007-0326-1_1.

McCormack, J., et al. (2017). Comparison of mesospheric winds from a high-altitude meteorological analysis system and meteor radar observations during the boreal winters of 2009–2010 and 2012–2013 *J. Atmos. Sol-Terr. Phys.*, **154**, 132-166. doi: 10.1016/j.jastp.2016.12.007.

McDonald, S. E., F. Sassi, and A. J. Mannucci (2015). SAMI3/SD-WACCM-X simulations of ionospheric variability during northern winter 2009. *Space Weather*, **13**, doi:10.1002/2015SW001223.

McDonald, S.E. et al. (2018). Impact of non-migrating tides on the low latitude ionosphere during a sudden stratospheric warming even in January 2010. *J. Atmos. Sol-Terr. Phys.*, **171**, 188-200, doi:10.1016/j.jastp.2017.09.012.

Mendillo, M., H. Rishbeth, R. G. Roble, and J. Wroten (2002). Modelling F2-layer seasonal trends and day-to-day variability driven by coupling with the lower atmosphere. *J. Atmos. Sol. Terr. Phys*., **64**, 1911‑1931, doi: 10.1016/S1364-6826(02)00193-1.

Richards, P. G., J. A. Fennelly, and D. G. Torr (1994). EUVAC: A solar EUV flux model for aeronomic calculations, J. Geophys. Res., 99, 8981–8992, doi:10.1029/94JA00518.

Richmond, A. (1995). Ionospheric electrodynamics using magnetic APEX coordinates. *J. Geomag. Geoelectr.*, **47**, 191-212.

Sassi, F., H.-L. Liu, J. Ma, and R.R. Garcia (2013). The lower thermosphere during the northern hemisphere winter of 2009: A modeling study using high-altitude data assimilation products in WACCM-X. *J. Geophys. Res.*, **118**, 1-15, doi: 10.1002/jgrd.50632, 2013.

Sassi, F., H.-L. Liu, and J. T. Emmert (2016). Traveling planetary-scale waves in the lower thermosphere: Effects on neutral density and composition during solar minimum conditions. *J. Geophys. Res. Space Physics*, **121**, doi:10.1002/2015JA022082.

Solomon, S. C., and L. Qian (2005). Solar extreme-ultraviolet irradiance for general circulation models, *J. Geophys. Res.*, **110**, A10306, doi: 10.1029/2005JA011160.

Theurich, G. et al. (2016). The Earth system prediction suite. *Bull. Amer. Met. Soc.*, **97**, 1229-1247.

Weimer, D. R. (2005), Improved ionospheric electrodynamic models and application to calculating Joule heating rates, J. Geophys. Res., **110**, A05306, doi:10.1029/2004JA010884.

Woods, T. and G. Rottman, 2002. Solar ultraviolet variability over time periods of aeronomic interest, in *Atmospheres in the Solar System: Comparative aeronomy, Geophys. Monogr. Ser.,* **130**, edited by M. Mendillo, A. Nagy, and J.H. Waite Jr, pp 221-234, AGU, Washington, DC.

Zawdie, K. A., D. P. Drob, J. D. Huba, and C. Coker (2016), Effect of time-dependent 3-D electron density gradients on high angle of incidence HF radiowave propagation, *Radio Sci.*, **51**, 1131–1141, doi:10.1002/2015RS005843.

Zawdie, K. A., D. P. Drob, D. E. Siskind, and C. Coker (2017). Calculating the absorption of HF radio waves in the ionosphere, *Radio Sci.*, *52*, 767–783, doi:10.1002/2017RS006256.

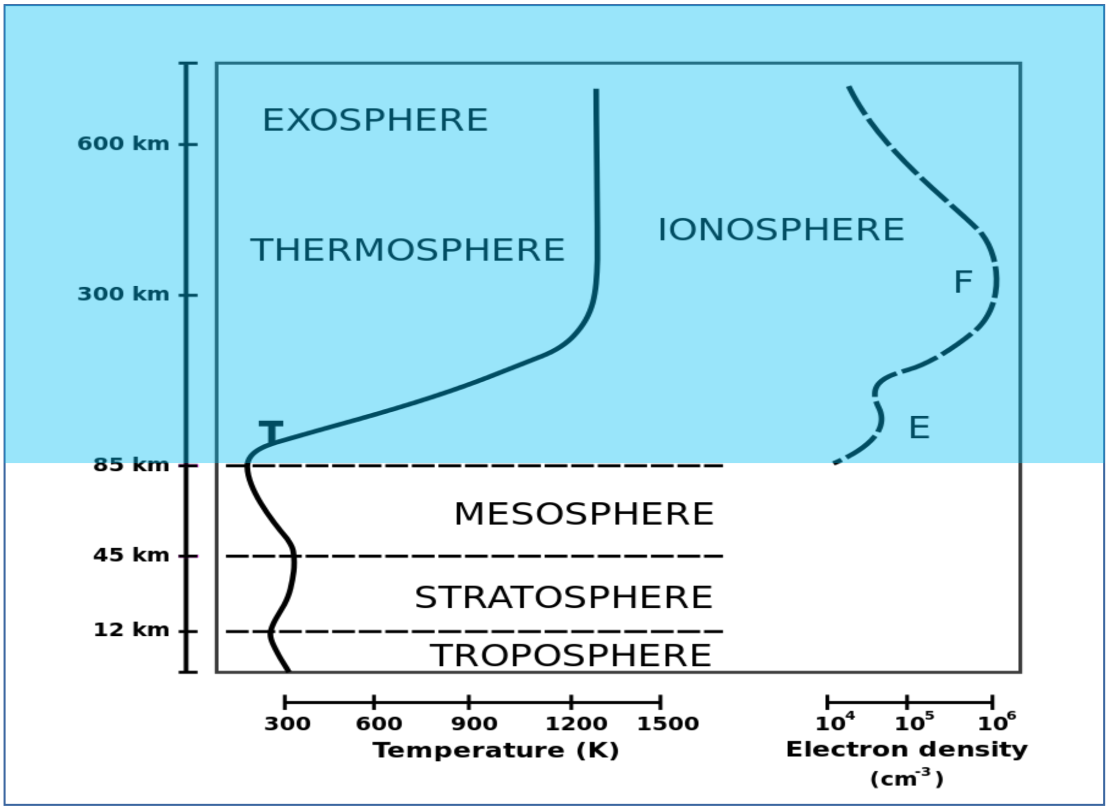

Figure 1. Schematics of the vertical structure of the atmosphere, from the ground to the exobase (~600 km). The light blue shade highlights the thermosphere and ionosphere mix above about 85 km.

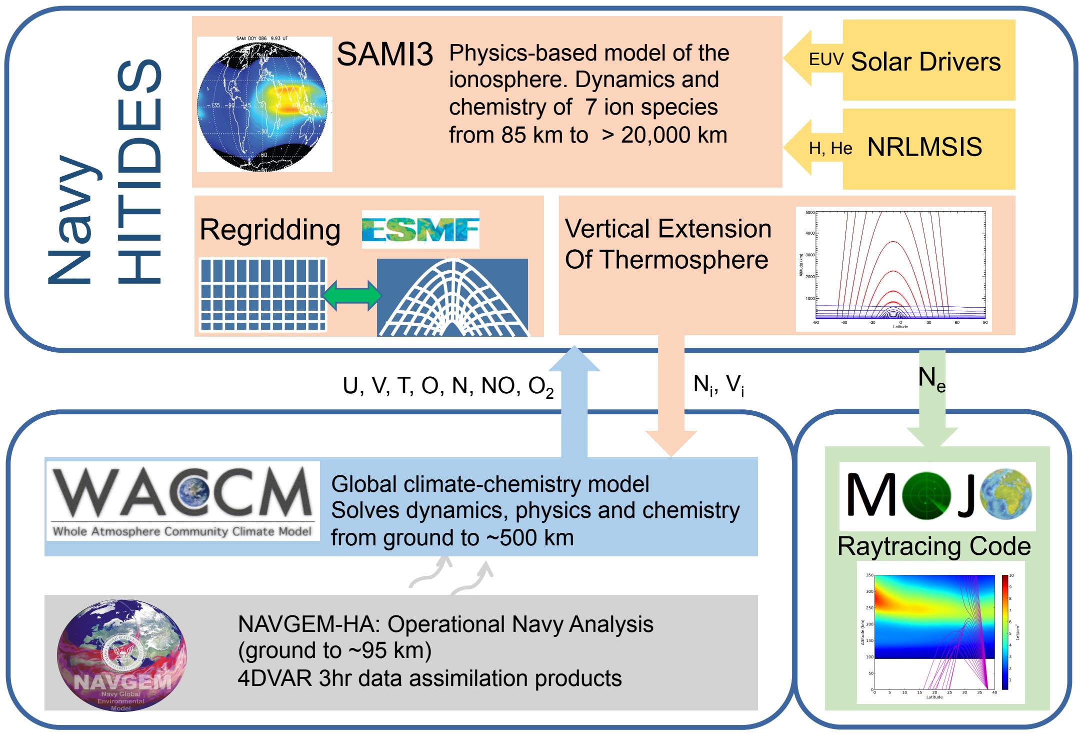

Figure 2. Schematic description of the two-way coupling between SAMI3 and WACCM-X, and how output from the coupled models may be used as input to the MoJo ray tracing code.

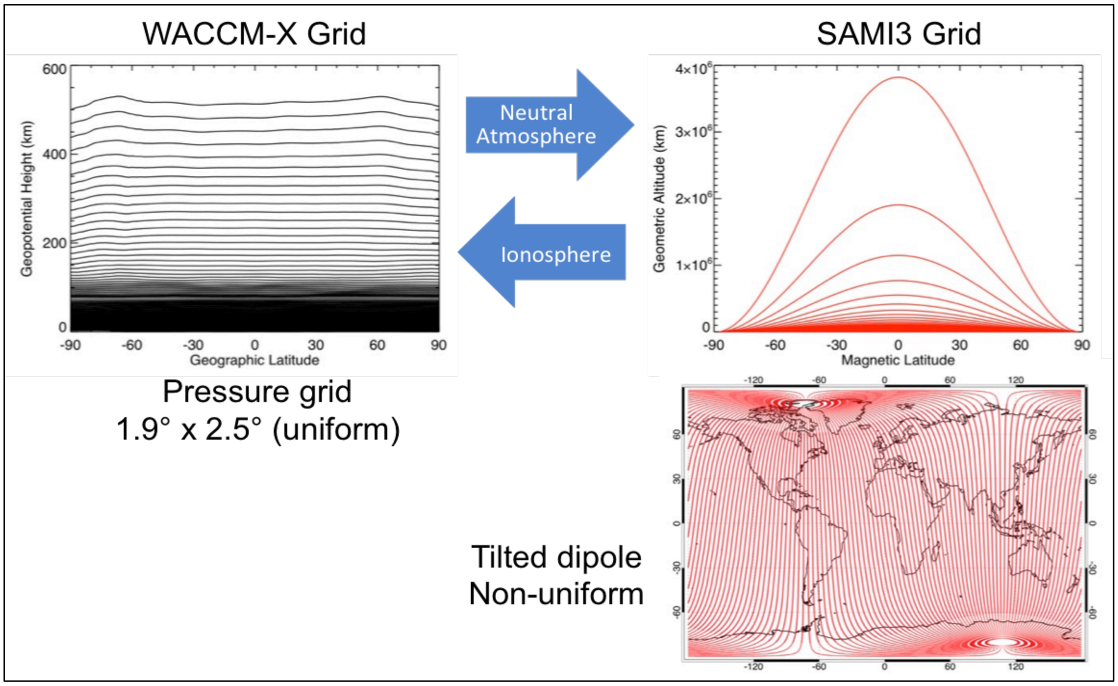

Figure 3. Top left: WACCM-X pressure levels for one longitude. Top right: SAMI3 magnetic field lines for one longitudinal slice. Bottom right: Global map of the SAMI3 magnetic field lines.

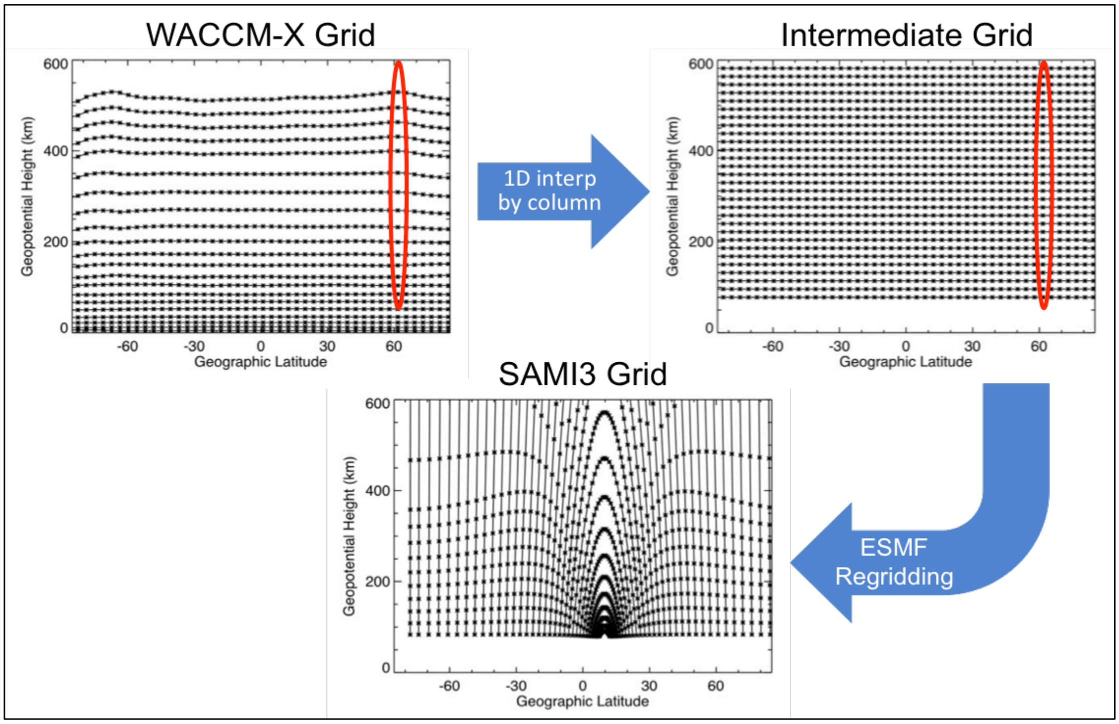

Figure 4. Schematic of the implementation of the ESMF regridding in Navy-HITIDES. Asterisks indicate individual grid points.

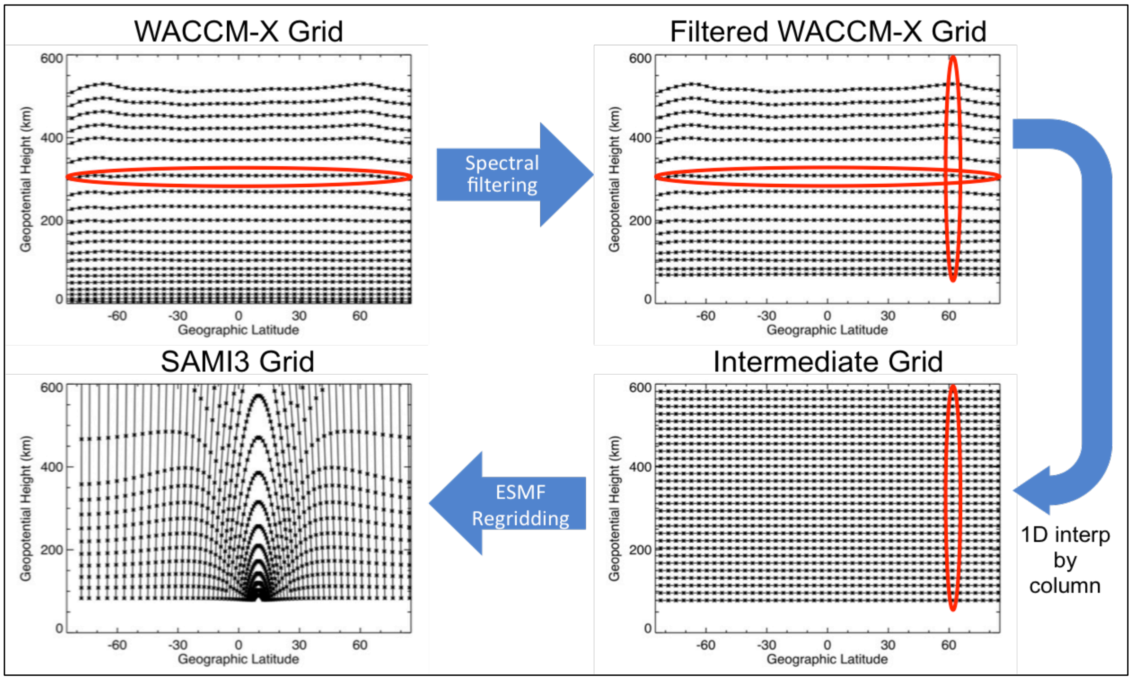

Figure 5. Schematic of the final implementation of the extension and re-gridding algorithm implemented in Navy-HITIDES.

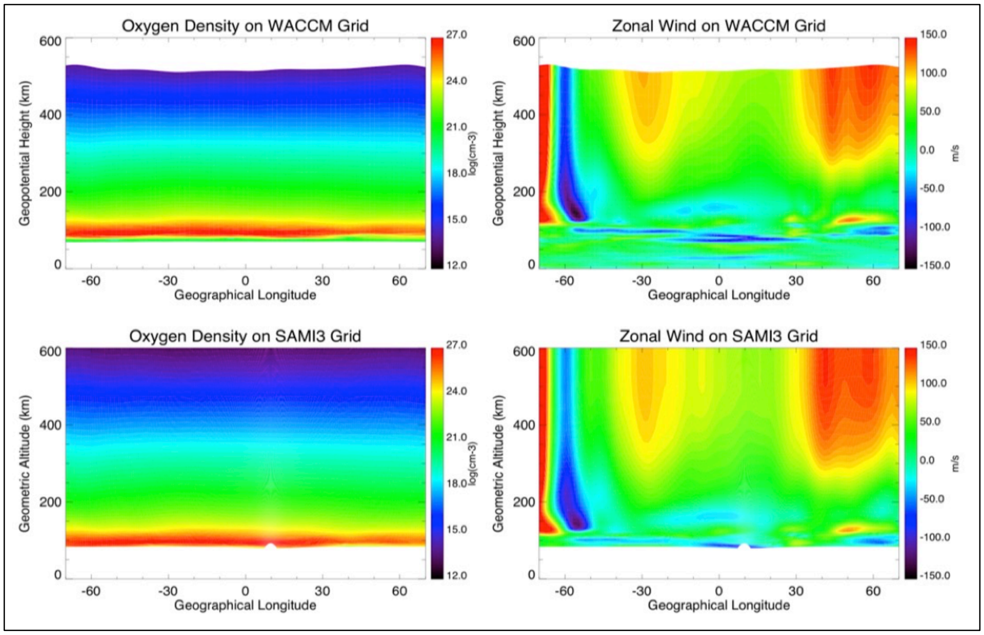

Figure 6. Results of the application of the interpolation and vertical extension algorithms: top row shows the WACCM-X fields; bottom row shows the results of the interpolation and extension. Left panels are the logarithm of the atomic oxygen, while right panels show the zonal wind. The WACCM-X fields are at longitude 117.5 degrees East and the interpolated fields are shown on the SAMI3 grid on field lines that most closely match the WACCM-X longitude.

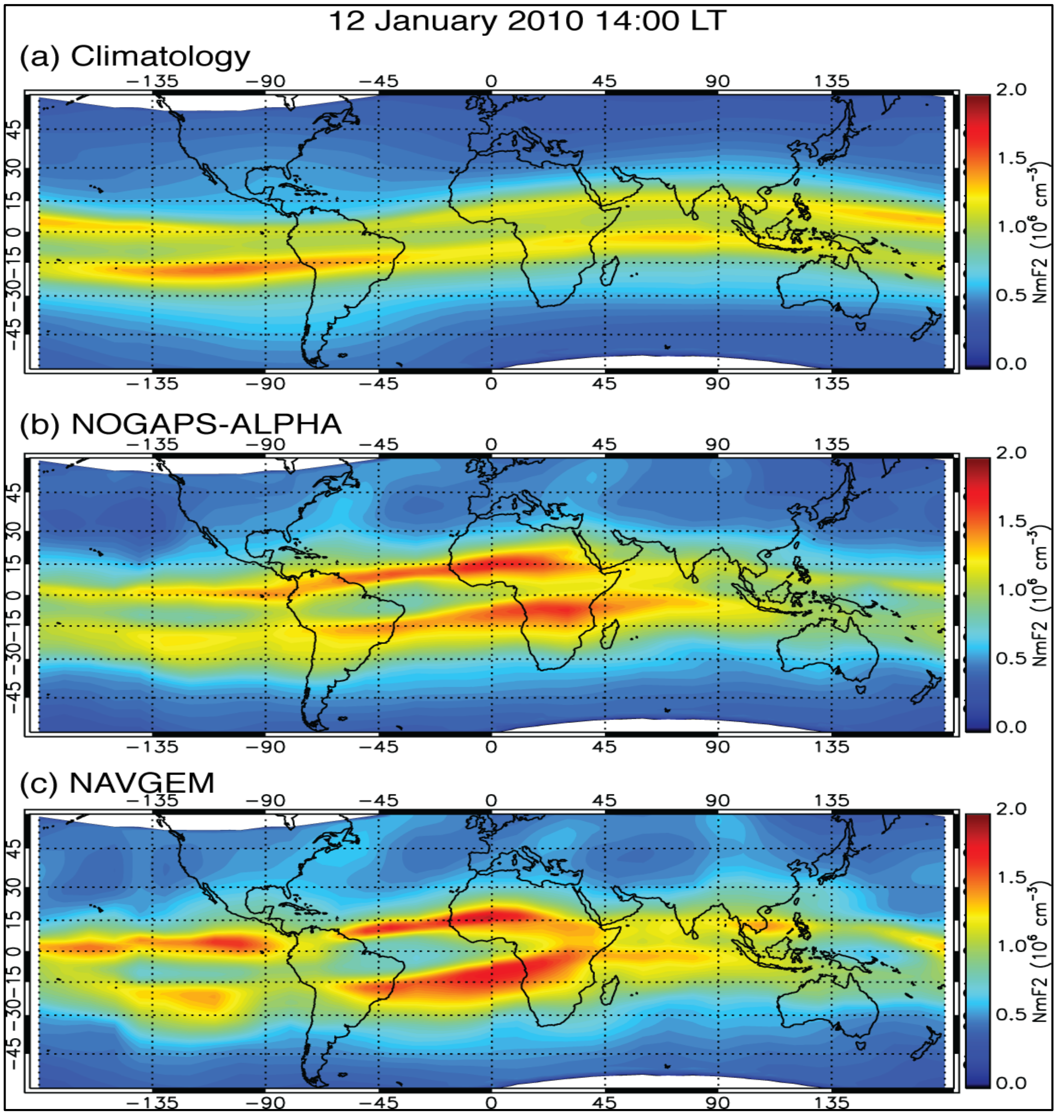

Figure 7. Peak electron density (NmF2) shown at a constant local time of 14:00 LT on 12 January 2010 using (a) climatological thermosphere from HWM14 and NRLMSIS, (b) thermosphere from WACCM-X forced with 6-hour NOGAPS-ALPHA data products and (c) thermosphere from WACCM-X forced with 3-hour NAVGEM-HA data products.

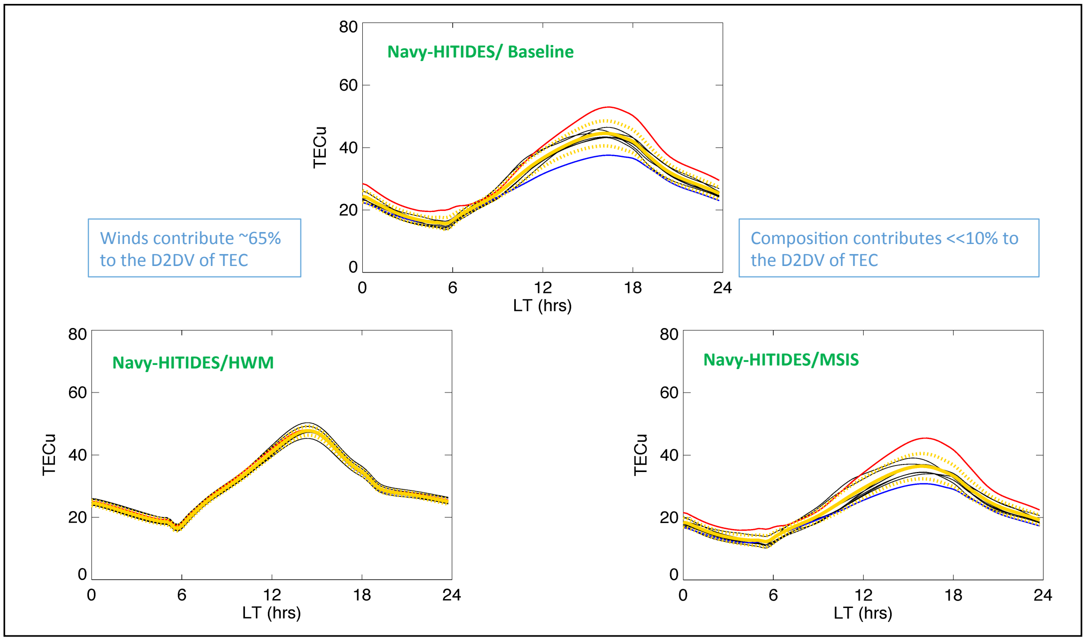

Figure 8. TEC from 11 January 2016 through 24 January 2016 as a function of local time (LT), averaged between longitudes 120W and 10W at 15S. Each black line corresponds to the TEC of one day; yellow solid line is the mean of all days; yellow dashed line represents the 1 standard deviation about the mean; red and blue lines are for two outlier days in the baseline simulation. Top row: Baseline simulation with meteorological drivers. Bottom row, LHS: Simulation uses winds from HWM in place of the day-to-day varying meteorological winds. Bottom row, RHS: Temperature and composition from MSIS replace the day-to-day varying meteorology.

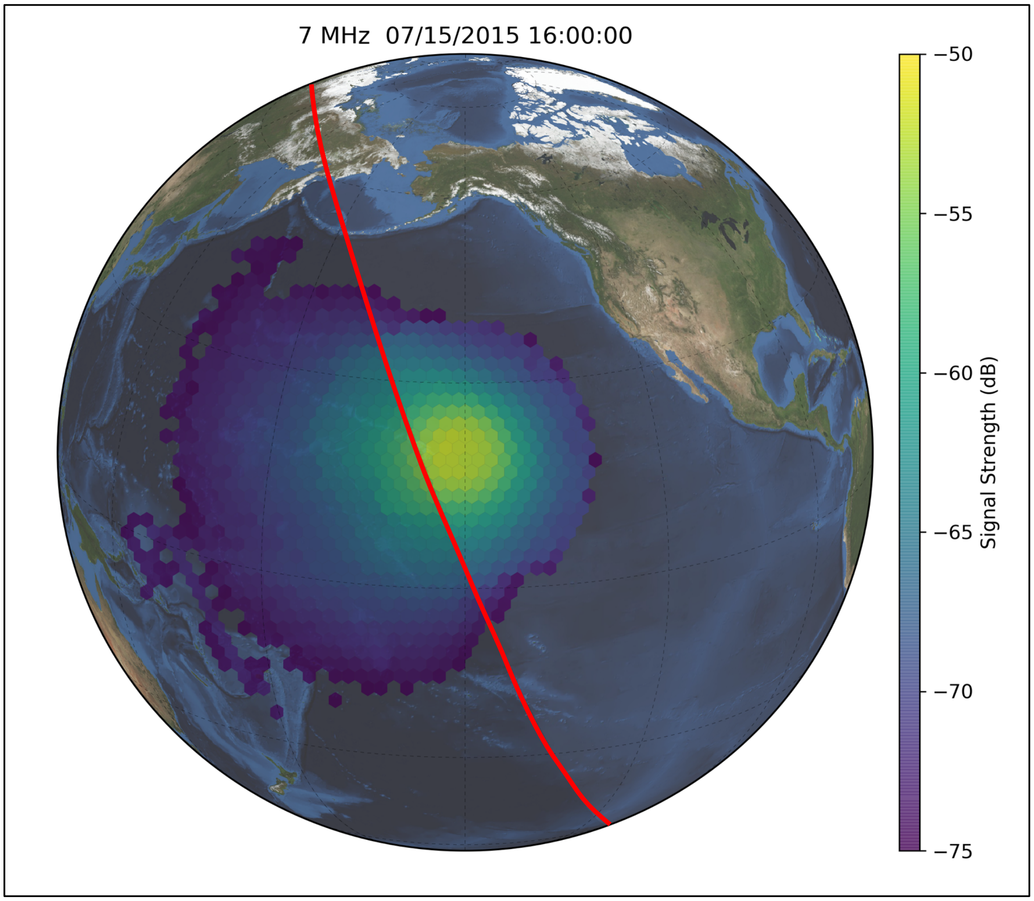

Figure 9. An example of signal strength (in dB) at 7 MHz simulated with the MoJo raytrace tool. The HITIDES electron density output was utilized as the ionosphere for this simulation, which demonstrates that changes in the ionosphere, such as the day/night terminator (red line), have a significant effect on signal strength.

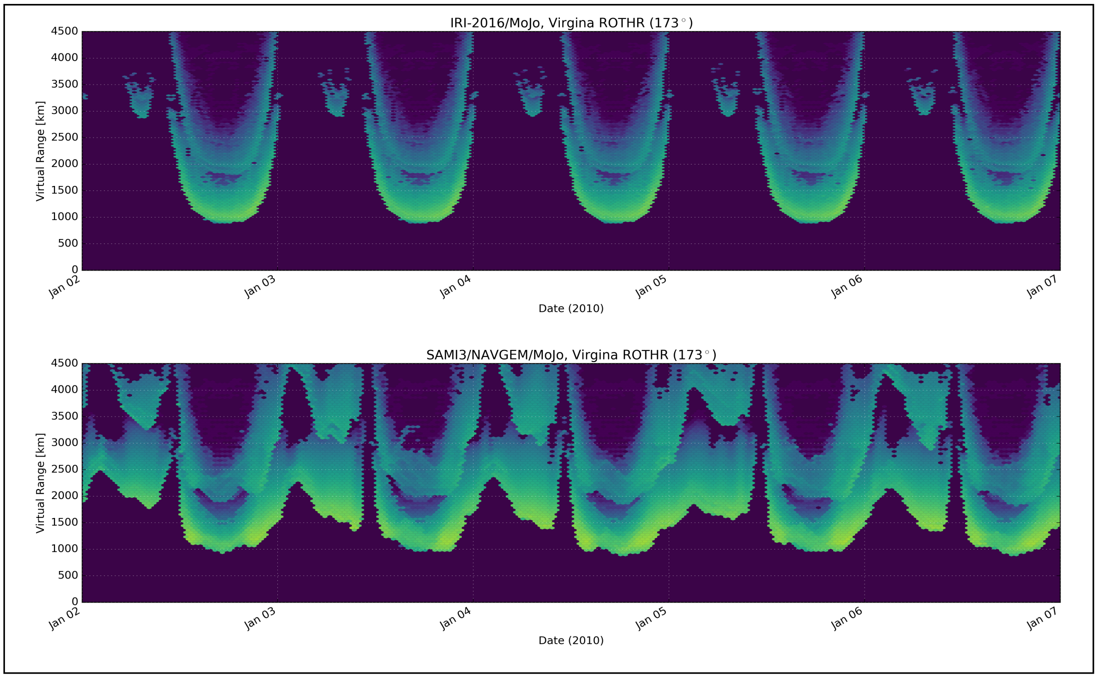

Figure 10. Simulated backscatter power for an OTHR as a function of time and virtual range. The top panel used a climatological model for the background ionosphere, the bottom panel used output from Navy-HITIDES and is better able to capture daily variations of the radar.

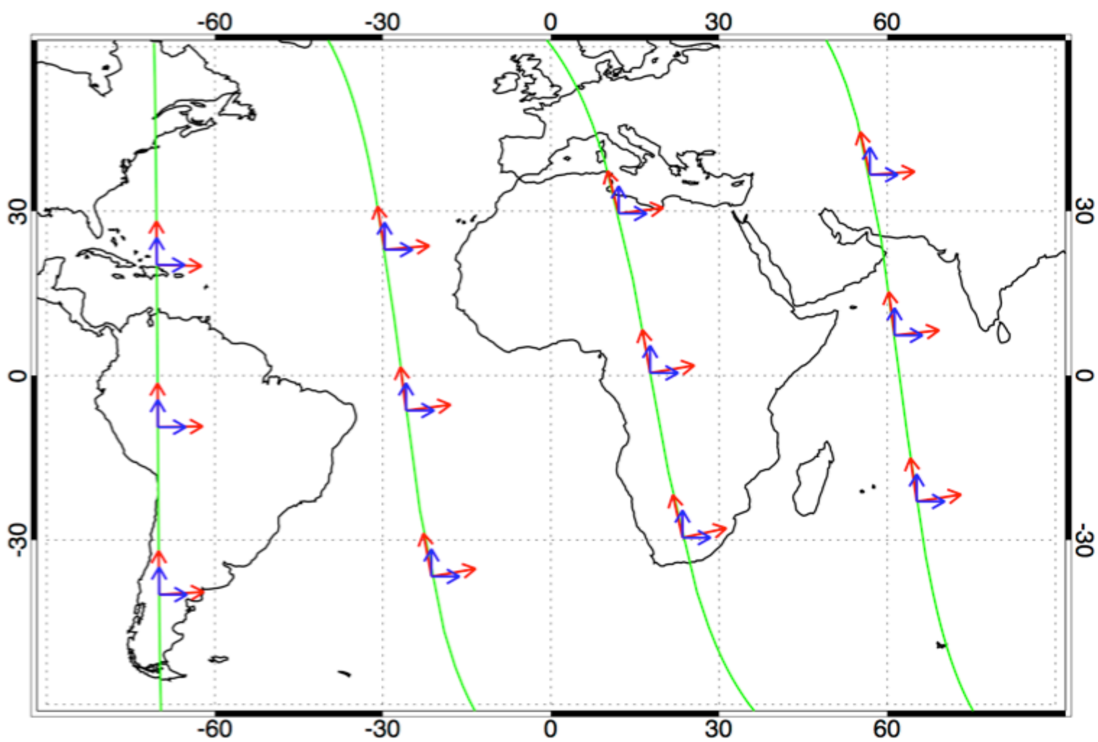

Figure 11. Map showing location dependent ionospheric **s** and **h** unit vectors (red arrows) and geographic **λ** and **φ** unit vectors (blue arrows). Magnetic field lines are shown in green.

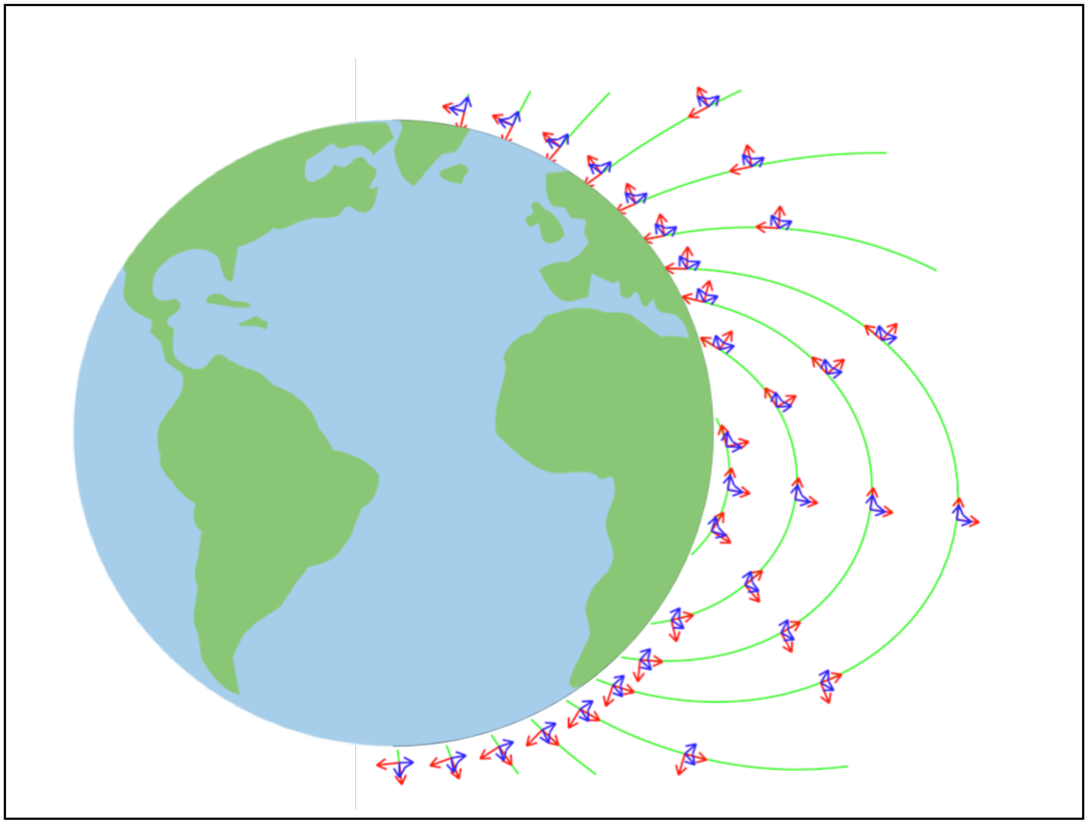

Figure 12. Schematic showing how ionospheric **s** and **p** unit vectors (red arrows) and geographic **λ** and **r** unit vectors (blue arrows) vary along the magnetic field lines (green lines).